THE JOURNAL OF PHYSICAL CHEMISTRY B

ARTICLE

pubs.acs.org/JPCB

Extreme-Values Statistics and Dynamics of Water at Protein Interfaces

Jean-Pierre Korb,[†] Yanina Goddard,[‡] Jason Pajski,[‡] Galina Diakova,[‡] and Robert G. Bryant*[,‡]

[†]Physique de la Matière Condensée, Ecole Polytechnique, CNRS, 91128 Palaiseau, France

[‡]Chemistry Department, University of Virginia, Charlottesville, Virginia 22904, United States

ABSTRACT: Immobilized proteins present a unique interface with water. The water translational diffusive motions affect the high-frequency dynamics and the nuclear spin−lattice relaxation as with all surfaces; however, rare binding sites for water in protein systems add very low-frequency components to the dynamics spectrum. Water binding sites in protein systems are not identical, thus distributions of free energies and consequent dynamics are expected. ^2H_2O spin−lattice relaxation rate measurements as a function of magnetic field strength characterize the local rotational fluctuations for protein-bound water molecules. The measurements are sensitive to dynamics down to the kilohertz range. To account for the data, we show that the extreme-values statistics of rare events, i.e., water dynamics in rare binding sites, implies an exponential distribution of activation energies for the strongest binding events. In turn, for an activated dynamical process, the exponential energy distribution leads to a Pareto distribution for the reorientational correlation times and a power law in the Larmor frequency for the ^2H_2O spin−lattice relaxation rate constants at low field strengths. The most strongly held water molecules escape from rare binding sites in times on the order of microseconds, which interrupts the intramolecular correlations and causes a plateau in the spin−lattice relaxation rate at very low magnetic field strengths. We examine the magnetic relaxation dispersion (MRD) data using two simple but related models: a protein-bound environment for water characterized by a single potential well and a protein-bound environment characterized by a double potential well where the potential functions for the local motions of the bound-state water are of different depth. This analysis is applied to D_2O deuterium spin−lattice relaxation on cross-linked albumin and lysozyme, which is dominated by the intramolecular relaxation driven by the dynamical modulation of the nuclear electric quadrupole coupling. We also separate the intramolecular from the intermolecular contribution to water proton spin−lattice relaxation by isotope dilution and show that the intramolecular proton data map onto the deuterium relaxation by a scale factor implied by the relative strength of the quadrupole and dipolar couplings. The temperature and pH dependence of the magnetic relaxation dispersion are complex and accounted for by changing only the weighting factors in a superposition of contributions from single-well and double-well contributions. These experiments show that the reorientational dynamics spectrum for water, in and on a protein, is characterized by a strongly asymmetric distribution with a long-time tail that extends at least to microseconds.

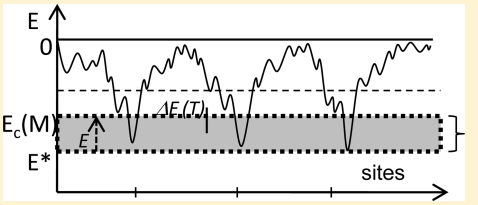

I. INTRODUCTION

Water is critical to biological viability and function at all levels of life. Except for portions of membrane-bound systems, water is the universal biological solvent; its interactions may modulate a variety of structural and energetic constraints associated with macromolecules and their assemblies. Water molecule dynamics affects the energetic as well as the steric aspects of both intra- and intermolecular processes; therefore, a more complete understanding of water molecule dynamics on these complex systems is crucial. Important components of the macromolecule and water dynamics occur at relatively low frequencies, the order of a catalytic rate constant, for example, even though critical motions may be affected by much faster events. The magnetic field dependence of nuclear spin−lattice relaxation rate constants, also called magnetic relaxation dispersion (MRD), is a powerful approach to characterization of dynamics.[1] The nuclear spin−lattice relaxation rate is proportional to the spectral power densities that are the Fourier transforms of the time correlation functions characterizing molecular motions. Nuclear spin−lattice relaxation rate constants are proportional to spectral density functions at the Larmor frequency and twice the Larmor frequency. Varying the magnetic field varies the Larmor frequency, and the spectral densities sampled thus provide a map of the molecular noise spectrum. A unique feature of MRD measurements is the sensitivity to dynamics that are slower than those readily accessible to most other methods such as molecular dynamics simulations, time domain infrared measurements, inelastic neutron scattering, and optical spectroscopy.[2−13]

Recent water−proton nuclear magnetic relaxation dispersion experiments (MRD) on protein solutions in the frequency range (30−500 MHz) have shown that the water-molecule-surface-average translational correlation time is 30−40 ps, and the shape of the dispersion profile is characteristic of two-dimensional diffusion of water in the protein interfacial region.[14] The short translational correlation time is consistent with rapid translational motions at the macromolecular surface usually observed in simulations. Because the nuclear spin-relaxation times are long, the total spin relaxation is often a weighted average over different

Received: June 7, 2011
Revised: September 20, 2011
Published: September 21, 2011

local dynamics, and a rare slow process may dominate the observation. ^{2}H and ^{17}O spin relaxation measurements are determined by intramolecular couplings that tie the measurements to rotational reorientation of the molecule. Because the magnetic moments are small, the intermolecular dipolar couplings that complicate ^{1}H measurements are insignificant. ^{17}O and ^{2}H spin relaxation studies also sample lower frequencies than ^{1}H measurements. Studies on immobilized protein systems at various temperatures and Larmor frequencies[15−18] have shown that the reorientational dynamics of the water molecules on the protein requires a power−law distribution of local correlation times to account for the data.[19] In the very high-frequency regime, molecular dynamics (MD) simulations have demonstrated a distribution of water molecule residence times at the protein−water interface.[20] These simulations have shown that the residence times of the interfacial water molecules depend upon the degree of exposure of the hydration sites to bulk solvent and that concave sites, buried cavities inside the protein, and grooves have longer residence times (t > 80 ps) than those that are convex and exposed to the bulk (t < 10 ps). On the other hand, MRD measurements have shown the existence of much longer lifetimes for specific, but rare, sites.[21−26] These sites are the class that are sometimes identified by water−protein proton nuclear Overhauser effects.[27,28] A significant distribution of water−molecule interactions and lifetimes in the interfacial region makes physical and chemical sense because of the surface roughness and chemical and steric heterogeneity. Nevertheless, a justification for a particular distribution has been so far elusive.

Our primary measurement here is the magnetic field dependence of the deuteron spin−lattice relaxation rate constant (MRD) in cross-linked lysozyme and bovine serum albumin (BSA) gels made in D_2O because this measurement isolates the reorientational dynamics of just water. Cross-linking the protein quenches the global rotation of the protein which permits examination of the dynamics slower than the rotational correlation time of the solution-phase protein. In companion measurements of the residual ^{1}H in D_2O, we have isolated the proton intramolecular contribution to the total water-proton relaxation rate constants by isotopic dilution. The intramolecular proton relaxation rate has the same magnetic field dependence as the deuterons. This agreement is critical and identifies chemical exchange of water from the protein to the bulk as the origin of the low-field MRD plateau observed for both nuclei.

To account for the $^{2}H_2O$ MRD, we start from the free energy profile represented in Figure 1 and find the probability distribution function (pdf) for the minima corresponding to strongly bound water in rare interfacial protein sites. We show that in the vicinity of the extrema, this pdf is given by Gumbel statistics,[29] i.e., the statistics of extreme values, so that the energies in this region are distributed exponentially. With the assumption of an exponential activation law for the local dynamics, this energy distribution leads directly to a Pareto distribution for the associated correlation times for molecular reorientation. This distribution function is applied to Lorentzian functions to deduce the spin-relaxation equation associated with the water−protein interface, which becomes a power−law in the Larmor frequency. We examine two cases corresponding to different values of the distribution exponent, α, for water in the protein interfacial domain. When α < 1, the average value of the reorientational correlation times diverges for an unbounded distribution, but it becomes finite if the range of the distribution is limited by a chemical event, which is chemical exchange from the protein to the bulk in the present cases. At long times (low frequency), this situation corresponds to spin relaxation dominated by the very few water molecules trapped in the deepest potential energy wells offered by the protein interface and influenced by the local fluctuations of the soft protein (Figure 1). On the other hand, when α > 1, the long-time tail of the distribution strongly attenuated, and the average value of the reorientational correlation time is close to the minimum value. This case describes the local reorientational dynamics of a second population of water in the interface that explores energetically higher regions of the free energy landscape. We apply this simplified approach to $^{2}H_2O$ MRD profiles as a function of temperature and show that the observed intramolecular water spin−lattice relaxation rates may be described by a linear combination of contributions from each class of binding sites with weighting coefficients that are temperature dependent. The upper bound for the correlation time distribution is associated with chemical exchange of water from the most strongly bound sites, which is practically independent of temperature. This unusual dependence is associated to the exchange determined by fluctuations in the protein structure, which in a fracton description are proportional to the temperature.[30]

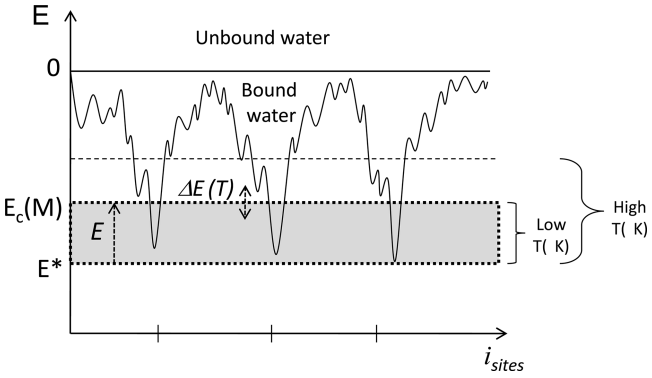

Figure 1. Schematic diagram of the rugged free energy landscape of the very large number of potential binding sites $i \in \{1,...,M\}$ for water in the interfacial domain of the immobilized protein. Here, $\Delta E(T)$ represents the temperature-dependent thermal fluctuations in a range of free energy around the deepest minima belonging to the shaded region when $E \rightarrow -\infty$.

The presentation is organized as follows: The first section introduces the ideas associated with the statistics of rare events as a foundation for understanding the low-frequency dynamics of water magnetic relaxation dispersion measurements in rotationally immobilized proteins. The second section provides experimental details. The third section outlines the application of extreme-values statistics to the theory of intramolecular nuclear spin relaxation induced by reorientational dynamics of water in protein binding sites. Two models are developed for water dynamics associated with single- and double-well potentials. The technical details about the extreme-values statistics and its application on MRD are collected in two appendices. The fourth section discusses the application of the theory to understanding the deuterium and proton MRD experiments. Finally, we summarize the main points of this study in the Conclusion.

II. EXPERIMENTAL SECTION

A. Materials. Bovine serum albumin (BSA Fraction V, Sigma-Aldrich, Inc., #A3059) or hen eggwhite lysozyme (HEWL) (Sigma Chemical Co., #L-6876) was dissolved in deionized water, then

dialyzed for 8 h against three changes of 4 L of water in a Spectra/Por membrane with a molecular weight cutoff of 6−8 kDa. The protein solutions were then lyophilized to constant weight. The protein was dissolved in 0.15 M sodium chloride solutions made using either H_2O or D_2O (99.9% D, Cambridge Isotope Laboratories, Andover, MA) and the isotope composition adjusted by volume.

BSA gels and HEWL gels were made by dissolving ∼1.5 g of protein in 9.0 mL of 0.15 M sodium chloride and distributing 0.9 mL aliquots into 10 mm glass tubes. The solutions were cooled on ice. An amount of 0.1 mL of cold 25% aqueous solution of glutaraldehyde (Sigma Chemical Co, St. Louis, MO) was added to each tube with vigorous stirring for two minutes. The gels were left to set overnight and then removed from the glass tubes and soaked in a 0.15 M sodium chloride solution of the desired hydrogen isotope composition. The gels were soaked in three successive 2 mL volumes of the appropriate proton mole fraction solution for a minimum of 3 h each. A second series of BSA gels were soaked for a total of eight cycles for a minimum of 24 h each.

B. Methods. The nuclear magnetic resonance data were recorded using a fast-field cycling NMR spectrometer FFC-2000 (Stelar s.r.l., Mede, Italy). Deuteron spins were polarized at a deuteron Larmor frequency of 5 MHz, and free induction decays were recorded following a single 28 μs 90° pulse applied at 5 MHz. The relaxation field Larmor frequencies were varied between 0.0015 and 5 MHz. The field-switching time was 3 or 4 ms. The NMR signal was averaged (24 scans) for 42 logarithmically spaced relaxation delay time sets, each of which was adjusted at every relaxation field to optimize the sampling of the decay/recovery curves. Within the experimental error, all the decay/recovery curves of longitudinal magnetization were exponential. Temperature was varied using the Stelar VTC90 variable-temperature controller, which was calibrated using an external thermocouple inserted into a surrogate sample at the resonance position in the probe. On the basis of repeated calibrations, the temperature in all NMR experiments was controlled within 0.5 K. The ^{1}H nuclear magnetic relaxation dispersion data were recorded with the same instrument. Spins were polarized at a Larmor frequency of 30 MHz and free-induction decays were recorded following a single 5.5 μs 90° excitation pulse applied at 15.8 MHz.

Figures 2 and 3 show the deuterium spin−lattice relaxation rate constants for water deuterons in cross-linked albumin and lysozyme as a function of magnetic field strengths at several temperatures. These rate constants are independent of magnetic field strength at low fields; i.e., there is a low-field plateau followed by a transition region to a high-field dependence that is a power−law in the Larmor frequency. The deuterium relaxation rate constants are determined by the reorientation of the electric field gradient associated with the OD bond in the water molecules. Intermolecular magnetic dipolar interactions with protons are weak by comparison to the intramolecular nuclear electric quadrupole contributions to relaxation. Thus, deuterium spin relaxation is different from proton relaxation that includes both intermolecular and intramolecular dipole−dipole contributions. The proton spin relaxation may derive from the interaction of the pair of water protons on the same molecule or from interactions of these protons with other water molecule protons or protein protons. The different ^{1}H contributions may be obtained by taking the difference between the total proton relaxation rate constant obtained in H_2O and that obtained for the residual protons in D_2O solutions which are dominated by the intermolecular contribution only.

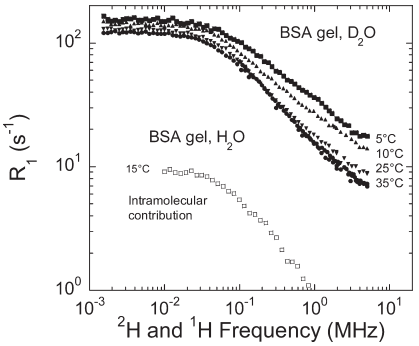

Figure 2. Deuteron spin−lattice relaxation rate as a function of the magnetic field strength plotted as the deuteron Larmor frequency for 15% BSA gel in D_2O at pH = 6 and at 5, 10, 25, and 35 °C, respectively, top to bottom. We have also displayed (□) the intramolecular contribution of the proton spin−lattice relaxation rate as a function of the magnetic field strength represented as the proton Larmor frequency for the same BSA gel in H_2O at 15 °C.

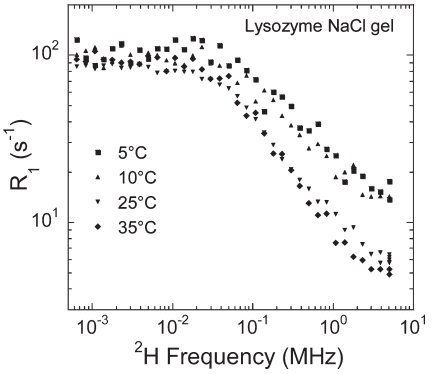

Figure 3. Deuteron spin−lattice relaxation rate as a function of the magnetic field strength plotted as the deuteron Larmor frequency for lysozyme gel in D_2O at 5, 10, 25, and 35 °C, respectively, top to bottom.

The intramolecular proton contributions to proton relaxation are summarized in Figure 2. Except for a scale factor associated with the difference in the strengths of the dipolar and quadrupolar couplings, the magnetic field dependence is the same for both nuclei; i.e., the high-field region is a power−law in the Larmor frequency; the low-field region is a plateau; and the transition between the two occurs at the same frequency within experimental error for both nuclei. We emphasize that the intramolecular ^{1}H relaxation is fundamentally different from that observed for protein protons or for the total water-proton relaxation rates in such gels that have often dominant contributions from intermolecular dipolar couplings to the rotationally immobilized protein protons. The protein-proton relaxation rate constants are described by a power−law in the Larmor frequency with an exponent of −0.78.[30−32] The intramolecular contribution, which results from the dipolar coupling between the two water protons, and deuterium relaxation shown in Figures 2 and 3 are described by smaller values. We seek to understand the origin of this power law. We note that magnetic field dependences similar to those reported here may derive from purely translational motions, even for the intramolecular relaxation problem of deuterium as developed earlier by Kimmich et al.[15−18] That model is of great interest in a number of high surface area

systems. Our concern with this model here is that the efficient diffusion of water in the interfacial region, which is approximately spherical, will average the correlation over a sphere in times much shorter than the reciprocal of the Larmor frequencies sampled here.

The protein has rare long-lived bound-water sites corresponding to the deep wells of Figure 1.[23−25,33,34] These rare sites may have significant water−protein proton nuclear Overhauser effects as noted by the Wuthrich laboratory[27,28] and are important to understanding the low-field spin−lattice relaxation here. It has been shown that a power law in the MRD profile may result from a power−law distribution of correlation times.[35] Now we examine the origins of this distribution and show how this may arise from the energetic characteristics of the water−protein interface.

III. THEORY

A. Statistics of the Binding Sites with the Deepest Potential. We consider the long-time or low-frequency dynamics of water at an interface and how it is affected by the rare transitions between the deepest minima represented by the shaded area of Figure 1. For the water−protein case, the deepest wells correspond to long-lived or trapped water on or within the folded structure of the protein, i.e., when the molecules explore the region around $E \rightarrow -\infty$ (shaded region of Figure 1). This problem is similar to the model developed by Bouchaud for studying low-temperature physics of disordered systems at equilibrium.[36]

Consider M-independent, identically distributed random variables (energies) $E = E_i$, $i \in \{1,...,M\}$, such that the probability distribution function (pdf) decays, for $E_i \rightarrow -\infty$, faster than any power law

$$p(E) = A \exp(-|E/E_0|^{\delta}) \tag{1}$$

Here $A = \delta/(2|E_0|\Gamma(1/\delta))$ is the normalizing constant ensuring that the integral of $p(E)$ over the free-energy range $\{-\infty < E < \infty\}$ is 1; E_0 represents a reference of free energy; the exponent $\delta > 0$; and Γ is the Gamma function. When the exponent δ satisfies the relation $0 < \delta < 1$, the form given in eq 1 is a stretched exponential. We show in Appendix A that δ must be greater than 1; thus, the form in eq 1 is different from a stretched exponential. For instance, for $\delta = 2$, one has a Gaussian pdf. The exact form of this pdf is not critical, but it should decay much faster than any power law.

We are interested in the statistics of the lowest free energy states $E^* = \min\{E_1,...,E_i,...,E_M\}$ for a very large ensemble of M random variables E_i. We show in Appendix A that the values of the extreme minima E^* fluctuate around some negative free energy, $E_c(M)$ (a bound state), defined by

$$E_c(M) \approx -E_0(\ln(M))^{1/\delta} \tag{2}$$

where the size of the fluctuations $\Delta E_c(M)$ around such a free energy $E_c(M)$ is given by

$$\Delta E_c(M) = E_0\frac{(\ln(M))^{(1-\delta)/\delta}}{\delta} \tag{3}$$

We see from eq 3 that for a very large number of M random variables $E_i (M \rightarrow \infty)$, the size of the fluctuations tends to zero when $\delta > 1$ and diverges if $\delta < 1$.

We show in Appendix A that the rescaled dimensionless minimum energy variable u

$$u = \frac{E^* - E_c(M)}{\Delta E_c(M)} \tag{4}$$

obeys, for large M, the universal Gumbel distribution[29]

$$p_M(u) = \frac{1}{\Delta E_c(M)} \exp[u - \exp(u)] \tag{5}$$

The maximum of this double exponential distribution occurs at $u = 0$ (Figure A1), which shows that $E_c(M)$ is the most probable value for the extreme (minimum) free energy. As in any "central-limit" theorem, this distribution is stable within a region where the deviation from $E_c(M)$ stays of the order of the relative fluctuations $|\Delta E_c(M)/E_c(M)| \approx 1/\ln(M)$ which goes to zero when $M \rightarrow \infty$ if $\delta > 1$ and diverges otherwise. A very important property of the Gumbel distribution is that it becomes a single exponential when the rescaled variable $u \rightarrow -\infty$ or $|\Delta E_c(M)| \rightarrow 0$ (see Figure A1)

$$p_M(u) \approx \frac{1}{\Delta E_c(M)} \exp[u] \tag{6}$$

In consequence, the low-lying energies, $E_i = E_c(M) + \Delta E_c(M)u_i$ with $i \in \{1,...,M\}$, displayed in Figure 1, are independent random variables that are exponentially distributed at the vicinity of the minima. We introduce the free energy barrier, $E = E_c(M) - E_i$, as the relative depth of the trap in Figure 1 and $\Delta E(T) \equiv \Delta E_c(M)$ as the average free energy of E due to the fluctuations. These fluctuations depend on temperature and on the heat capacity C_v through the relation

$$\sqrt{\langle \Delta E(T) \rangle^2} = \sqrt{kT(C_v T)} \tag{7}$$

If the heat capacity is practically constant over a temperature range, then $\Delta E(T)$ varies linearly with temperature in this range. The normalized pdf, $p(E)$, of the free energy landscape around such low-lying energies thus becomes an exponential function

$$p(E) = \frac{1}{\Delta E(T)} \exp\left(-\frac{E}{\Delta E(T)}\right) \tag{8}$$

where the integration over all the free energy barriers of the bound states, $\int_0^\infty p(E)\mathrm{d}E = 1$, ensures the normalization of the pdf $p(E)$.

B. Pareto Distribution of Reorientational Correlation Times of Water in the Deepest Potential Binding Sites. In the coarse-grained description presented in Figure 1 (dashed region), only the water molecules highly trapped in the deepest bounded free energy minima E_i will govern spin relaxation caused by the water reorientational dynamics at long times and low magnetic field strengths. We consider the general problem of a water molecule that reorients randomly within a landscape of potential wells of depth, E, that corresponds to the relative free energy barrier defined in eq 8. The exponential form chosen for $p(E)$ fulfills the physical condition that deep potentials wells are a priori rare.

We simplify the problem and suppose that each water molecule trapped in a well of depth E can reorient in such a trap with a rate constant, $r_{reor} \propto \exp(-E/RT)$; i.e., the reorientation is an activated process. As a result, the mean waiting time to

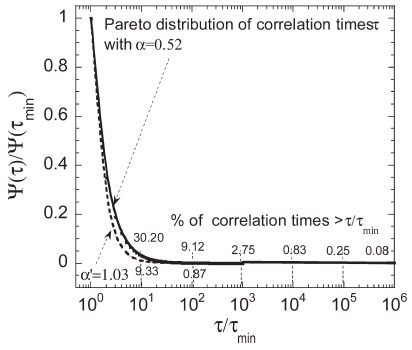

Figure 4. Calculated time dependences of the normalized Pareto distribution $\Psi(\tau)/\Psi(\tau_{min})$ with the reduced time scale τ/τ_{min} for two different values $\alpha = 0.52$ and $\alpha' = 1.03$. We indicate the percentage of correlation times calculated with eq 15 longer than a certain limit labeled above or below the continuous curves.

reorient, τ, is

$$\tau = \tau_{min} e^{E/kT} \approx 1/r_{reor} \tag{9}$$

where τ_{min} is a characteristic time.

The probability density function for waiting time $\Psi(\tau)$ between molecular reorientations satisfies the conservation equation

$$\Psi(\tau)d\tau = p(E)dE \tag{10}$$

This equation relates the free energy landscape around the extrema (minima) to the correlation−time scale; i.e., the deeper the well the longer the correlation time. Substituting eqs 8 and 9 into eq 10 leads to a Pareto distribution for

$$\Psi(\tau) = \frac{\alpha \tau_{min}^{\alpha}}{\tau^{1+\alpha}} \tag{11}$$

where $\int_{\tau min}^{\infty} \Psi(\tau)d\tau = 1$; τ_{min} appears as a time cutoff at short time; and according to eq 10 and eq 11 α is the Pareto exponent defined as

$$\alpha = \frac{kT}{\Delta E(T)} \tag{12}$$

From eq 7, the thermal fluctuations of free energy vary linearly with the temperature, $\Delta E(T) \propto kT$, and according to eqs 12 and 7, α is independent of temperature unless as noted earlier the system heat capacity is temperature dependent. We return to this point in Section IV. We show in Figure 4 the normalized Pareto distribution $\Psi(\tau)/\Psi(\tau_{min})$ as a function of the reduced correlation time, τ/τ_{min}, for two values of α: ($\alpha < 1$ and $\alpha > 1$). In the case that the correlation time is bounded, $\tau_{min} \leq \tau \leq \tau_{max}$ with $\tau_{min} \ll \tau_{max}$, we may generally compute the average reorientational correlation time $<\tau>$ defined as the first moment of the Pareto distribution (eq 11)

$$\langle\tau\rangle = \frac{\alpha}{1-\alpha}\tau_{min}\left[\left(\frac{\tau_{max}}{\tau_{min}}\right)^{1-\alpha} - 1\right] \tag{13}$$

When $\alpha < 1$, this average is finite but much larger than τ_{min}. For instance, when $\alpha = 0.52$, $\tau_{min} \approx 1$ ps, and $\tau_{max} \approx 3$ μs, one finds $<\tau> = 1392\tau_{min}$. For this condition, there is a very long-time tail for the Pareto pdf, and in the limit that $\tau_{max} \rightarrow \infty$, the average $<\tau>$ even diverges. However, when $\alpha > 1$, this average is of the order of a few τ_{min}

$$\langle\tau\rangle = \frac{\alpha}{\alpha-1}\tau_{min}\left[1 - \left(\frac{\tau_{min}}{\tau_{max}}\right)^{\alpha-1}\right] \approx \frac{\alpha}{\alpha-1}\tau_{min} \tag{14}$$

For example, when $\alpha = 1.03$, one finds from eq 14 $<\tau> = 34\tau_{min}$.

It is useful to estimate the probability $P_{rest}(\alpha, \tau_{limit})$ to have a correlation time τ larger than a certain time limit $\tau_{limit} \gg \tau_{min}$, from the Pareto distribution (Figure 4). This probability is given by

$$P_{rest}(\alpha, \tau_{limit}) = 1 - \int_{\tau_{min}}^{\tau_{limit}} \Psi(\tau')d\tau' = \left(\frac{\tau_{min}}{\tau_{limit}}\right)^{\alpha} \tag{15}$$

We have indicated in Figure 4 the value of the percentage of correlation times larger than a certain time limit $100\% \times P_{rest}(\alpha, \tau_{limit})$. If we assume that ≈1500 water molecules are transiently present in the hydration domain at the protein interface, $1500 \times P_{rest}(\alpha, \tau_{limit})$ approximates the number of remaining highly trapped water molecules with a correlation time $\tau > \tau_{limit}$. For $\alpha = 0.52$, this relation gives 12, 4, or ≈1 water molecules for $\tau_{limit} \geq 10^4 \times \tau_{min}$, $10^5 \times \tau_{min}$, and $\tau_{max} \approx 10^6 \times \tau_{min}$, respectively. These numbers show clearly that the low-frequency behavior of the spin−lattice relaxation rate is dominated by extremely rare sites characterized by long reorientational correlation times.

C. Theory of Intramolecular NMRD Induced by Reorientational Dynamics of Water at Protein Binding Sites. To interpret the deuteron NMRD data obtained in the case of protein gel in D_2O, we apply the fast exchange model where the total spin−lattice relaxation rate $R_{1Q,intra}$ is a superposition of population-weighted contributions from the bulk and protein interface contributions

$$R_{1Q,intra}(\omega_0) \approx R_{1Q,Bulk} + R_{1Q,Surf\text{-}intra}(\omega_0) \tag{16}$$

The bulk contribution $R_{1Q,Bulk}$ is a constant in the frequency range studied because the reorientation correlation time is very short compared with the inverse of the Larmor frequency.[37] The surface contribution $R_{1,Surf\text{-}intra}(\omega_0)$ for a nuclear spin $I = 1$ is given formally by the linear combination of surface spectral density functions $<j_{Q,Surf\text{-}intra}(\omega)>_{\psi}$ averaged over the Pareto distribution of correlation times given in eq 11

$$R_{1Q,Surf\text{-}intra}(\omega_0) \propto \frac{3}{80}p_B[\langle j_{Q,Surf\text{-}intra}(\omega_0)\rangle_{\Psi} + 4\langle j_{Q,Surf\text{-}intra}(2\omega_0)\rangle_{\Psi}] \tag{17}$$

Here p_B is the probability for D_2O to be in the protein interface domain. To estimate the spectral density function $<j_{Q,Surf\text{-}intra}(\omega_0,\tau)>_{\psi}$ for the reorientational dynamics of the D_2O at the bound site, one should know first the form of the time dependence of the reorientation correlation function $G_{Q,Surf\text{-}intra}(t)$ describing the quadratic fluctuations of the axial electric field gradient tensor. Guided by our observations, we consider the two following models for water motions in the rare protein-bound sites.

1. Single-Well Case. For the single-well case appropriate to low temperature, the water molecules are presumed to experience some restricted local reorientational motion permitted by the constraints imposed by the walls of the rare bound-state cavity. We assume that the bound D_2O senses a single quadrupole coupling constant and a local small angle reorientation driven by

the local thermal fluctuations of the bound environment. One may assume, in this case, an exponential correlation function $G^{\text{Single well}}_{Q,\text{Surf-intra}}(t) \approx \omega_Q^2 \exp(-|t|/\tau)$, scaled by an orientational order parameter $S^2 < 1$ that leads to the Lorentzian spectral density of the form $j^{\text{Single well}}_{Q,\text{Surf-intra}}(\omega_0) = \omega_Q^2 2\tau/(1 + \omega_0^2\tau^2)$. Here $\omega_Q = (2\pi e^2 qQ/h)$ is the deuterium quadrupole coupling constant for D_2O. To take into account the diversity of correlation times, τ, sampled by the bound-state water population, we evaluate the $\langle j^{\text{Single well}}_{Q,\text{Surf-intra}}(\omega_0)\rangle_\Psi$ of individual spectral density over the Pareto distribution $\Psi(\tau)$ of correlation times given in eq 11

$$\langle j^{\text{Singlewell}}_{Q,\text{Surf-intra}}(\omega_0)\rangle_\Psi = 2\omega_Q^2 \int_{\tau_{\min}}^{\tau_{\max}} \frac{\tau}{1 + \omega_0^2\tau^2}\Psi(\tau)\mathrm{d}\tau$$
$$= \frac{2\omega_Q^2 \alpha}{1-\alpha}\tau_{\min}\left[\left(\frac{\tau_{\max}}{\tau_{\min}}\right)^{1-\alpha} f(\alpha,\omega_0,\tau_{\max}) - f(\alpha,\omega_0,\tau_{\min})\right] \quad (18a)$$

with

$$f(\alpha,\omega_0,\tau_{\max}) \equiv {}_2F_1\left(1,\frac{1-\alpha}{2},\frac{3-\alpha}{2},-\omega_0^2\tau_{\max}^2\right) \quad (18b)$$

where the hypergeometric function ${}_2F_1$ can be calculated numerically either by a series or by an asymptotic expression. Substitution of eqs 18a and 18b) into eq 17 gives

$$R^{\text{Singlewell}}_{1Q,\text{Surf-intra}}(\omega_0) = \frac{3}{80}p_B\omega_Q^2\frac{2\alpha}{1-\alpha}\tau_{\min}\left\{\left(\frac{\tau_{\max}}{\tau_{\min}}\right)^{1-\alpha} f(\alpha,\omega_0,\tau_{\max})\right.$$
$$\left. - f(\alpha,\omega_0,\tau_{\min}) + 4\left[\left(\frac{\tau_{\max}}{\tau_{\min}}\right)^{1-\alpha} f(\alpha,2\omega_0,\tau_{\max}) - f(\alpha,2\omega_0,\tau_{\min})\right]\right\} \quad (19)$$

This expression has the following analytical limits

$$R^{\text{Singlewell}}_{1Q,\text{Surf-intra}}(\omega_0 \to 0) \approx \frac{3}{8}p_B\omega_Q^2\frac{\alpha}{1-\alpha}\tau_{\min}\left[\left(\frac{\tau_{\max}}{\tau_{\min}}\right)^{1-\alpha} - 1\right]$$
$$= \frac{3}{8}p_B\omega_Q^2\langle\tau\rangle \quad (20a)$$

$$R^{\text{Singlewell}}_{1Q,\text{Surf-intra}}(\omega_0 >> 1) \approx \frac{3\pi}{80}p_B\omega_Q^2\alpha(1 + 2^{1+\alpha})\sec\left(\frac{\alpha\pi}{2}\right)$$
$$\times \tau_{\min}\frac{1}{(\omega_0\tau_{\min})^{1-\alpha}} \quad (20b)$$

where the average correlation time $<\tau>$ is defined in eq 13. For this model in the low field limit, $R^{\text{Single well}}_{1Q,\text{Surf-intra}}$ is a constant proportional to the average correlation time that increases in proportion to $\tau_{\min}(\tau_{\max}/\tau_{\min})^{1-\alpha}$. As shown in Section III, this low-field relaxation rate is determined by the very few, about $1500 \times P_{\text{rest}}(\alpha,\tau \approx \tau_{\max})$, strongly trapped water molecules with a correlation time close to the long time limit, $\tau \approx \tau_{\max}$. In the high magnetic field limit, the relaxation rate is a power law in the Larmor frequency, $R^{\text{Single well}}_{1Q,\text{Surf-intra}} \propto 1/\omega_0^{1-\alpha}$, that yields the Pareto exponent α from the experimental MRD profile. Finally, the temperature dependence one deduces from eqs 20a and 20b is

$$R^{\text{Singlewell}}_{1Q,\text{Surf-intra}}(\omega_0,T) \propto \tau^{\alpha}_{\min}(T) \quad (21)$$

over the whole frequency range where we assume that $\tau_{\max}$ is a weak function of temperature as required by the data and

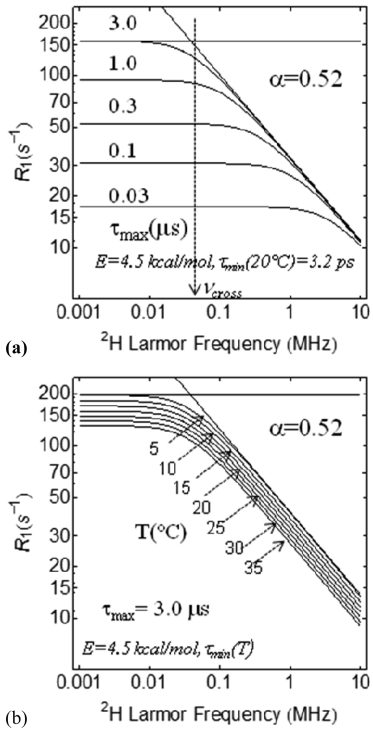

Figure 5. (a) Calculated frequency dependencies of $R^{\text{Single well}}_{1Q,\text{Surf-intra}}(\omega_0,T)$ obtained from eq 19 with $\alpha = 0.52$ at 20 °C when varying $\tau_{\max} \in \{0.03 - 3.0\ \mu s\}$ upward for a fixed $\tau_{\min} = 3.2$ ps at $T = 25$ °C. We have also displayed the calculated low- and high-frequency analytical limits given in eqs 20a and 20b, respectively. (b) Calculated frequency dependencies of $R^{\text{Single well}}_{1Q,\text{Surf-intra}}(\omega_0,T)$ obtained from eq 19 with $\alpha = 0.52$ and varying $\tau_{\min}(T)$ in the range 5−35 °C for a fixed value of $\tau_{\max} \approx 1/(2\pi\nu_{\text{cross}}) = 3.0\ \mu s$ corresponding to the inverse of the crossover frequency $\nu_{\text{cross}} \approx 40$ kHz observed in Figures 2−4.

discussed below. Figure 5a shows the frequency dependence of $R^{\text{Single well}}_{1Q,\text{Surf-intra}}(\omega_0,T)$ obtained with eq 19 and $\alpha = 0.52$ calculated for two limiting situations: (i) $\tau_{\max} \in \{0.03 - 3.0\ \mu s\}$ is varied for fixed $\tau_{\min} = 3.2$ ps at $T = 20$ °C (Figure 5a); (ii) $\tau_{\min}\{T(5-35\ ^\circ\text{C})\}$ is varied for a fixed value of $\tau_{\max} \approx 1/(2\pi\nu_{\text{cross}}) = 3.0\ \mu s$ (Figure 5b) corresponding to the inverse of the crossover frequency $\nu_{\text{cross}} \approx 40$ kHz for the transition between the power law and plateau observed in Figures 2 and 3. The value of $\tau_{\min}(T)$ has been chosen with an activation energy $E = 4.5$ kcal/mol only slightly less than the bulk value of $E_{\text{bulk}} = 4.8$ kcal/mol. There are two points to make in the comparison of Figure 5 with Figures 2 and 3. (i) The low-field relaxation rate constant is not a strong function of temperature as it would be for the choice of Figure 5a. (ii) The frequency of the transition between the power law and the plateau region for all experiments performed is at most a weak function of temperature similar to that shown in Figure 5b. Thus, the data of Figures 2 and 3 are consistent with a conclusion that $\tau_{\max}$ is a weak function of temperature over the temperature range studied.

2. Double-Well Case. We consider the possibility that the water molecules in the rare strongly bound protein environments may jump between two local environments characterized by different activation barriers, one with a lower activation free energy $E' < E$ just above the shaded range of Figure 1. In this case, the water molecules experience two environments that may be characterized by different magnitudes of the quadrupole coupling

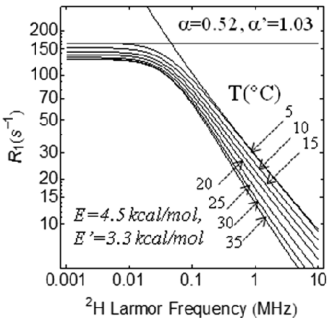

Figure 6. Calculated frequency dependences of $f(T)R_{1Q,\text{Surf-intra}}^{\text{Single well}}(\omega_0,T) + [1 - f(T)]R_{1Q,\text{Surf-intra}}^{\text{Double well}}(\omega_0,T)$ obtained with eqs 19 and 26 with $\alpha = 0.52$, $\alpha' = 1.03$, $E = 4.5$ kcal/mol, and $E' = 3.3$ kcal/mol for $T = 5-35$ °C.

constants ω_{Q1} and ω_{Q2} with $\omega_{Q1} < \omega_{Q2}$ because the magnitude is a function of the hydrogen-bond arrangement about the observed water molecule. Transitions between the populations in these two wells with activation energies E' and E, respectively (see Figure B1) add to the dynamics that drive the spin relaxation and change the averaged time-correlation functions that are recalculated in Appendix B yielding

$$\bar{G}_{Q,\text{Surf–intra}}^{\text{Doublewell}}(\tau) = \left[\omega_{Q1}\frac{\tau}{\tau + \tau'} + \omega_{Q2}\frac{\tau'}{\tau + \tau'}\right]^2 + |(\omega_{Q1} - \omega_{Q2})|^2\frac{\tau_p}{\tau + \tau'}e^{-\tau/\tau_p} \quad (22)$$

where the correlation times associated to these two wells are

$$\tau = \tau_0 \exp\left(\frac{E}{RT}\right)$$
$$\tau' = \tau_0' \exp\left(\frac{E'}{RT}\right) \quad (23)$$
$$\tau_p = \frac{\tau\tau'}{\tau + \tau'}$$

This correlation function tends to a quadratic residual quadrupolar term that is a time-weighted average of the two quadrupolar environments. The spectral density is obtained by the Fourier transform of eq 22, where one can omit the constant term

$$j_{Q,\text{Surf-intra}}^{\text{Doublewell}}(\omega_0) = 2|(\omega_{Q1} - \omega_{Q2})|^2\frac{1}{\tau + \tau'}\frac{\tau_p^2}{1 + \omega_0^2\tau_p^2} \quad (24)$$

This spectral density differs from the usual Lorentzian in that it has a different temperature dependence. The idea of the model is that the potential wells are of unequal depth, i.e., that $E > E'$ (Figure B1 of Appendix B). We assume that the transition rates defined in Appendix B satisfy the condition $W \ll W'$. In consequence, one has $\tau \gg \tau'$, and according to eq 23 $\tau_p \approx \tau'$. The different strongly bound water sites on the protein are undoubtedly different in local structure and free energy. Yet, the magnetic field dependence remains a power law which derives from the Lorentzian-like contributions of eq 24. Although it is possible to imagine different distribution functions for the local dynamical parameters, the power-law is preserved if we assume another Pareto distribution of correlation times $\Psi(\alpha',\tau')$ characterized by a Pareto exponent $\alpha' > 1$. Figure 4 shows that $\Psi(\alpha' > 1,\tau')$ decays much faster than $\Psi(\alpha < 1,\tau)$. For instance, for $\alpha' = 1.03$, only 9.33% of water molecules in the interface domain have a correlation time $\tau' \geq 10\tau'_{\text{min}}$ and only 0.87% for a correlation time scale $\tau' \geq 100\tau'_{\text{min}}$. We evaluate now $\langle j_{Q,\text{Surf-intra}}^{\text{Single well}}(\omega_0)\rangle_{\Psi,\Psi'}$ averaged over the two Pareto distributions $\Psi(\alpha < 1,\tau)$ and $\Psi'(\alpha' > 1,\tau)$

$$\langle j_{Q,\text{Surf}-\text{intra}}^{\text{Doublewell}}(\omega_0)\rangle_{\Psi,\Psi'} \approx 2|(\omega_{Q1} - \omega_{Q2})|^2\int_{\tau_{\text{min}}}^{\tau_{\text{max}}} d\tau\frac{\Psi(\tau)}{\tau} \times \int_{\tau'_{\text{min}}}^{\tau'_{\text{max}}} d\tau'\left(\frac{\tau'^2}{1 + \omega_0^2\tau'^2}\right)\Psi'(\tau')$$
$$\approx 2|(\omega_{Q1} - \omega_{Q2})|^2\frac{\alpha}{1 + \alpha}\left(\frac{\alpha'}{2 - \alpha'}\right)\frac{\tau'^2_{\text{min}}}{\tau_{\text{min}}} \times \left[\left(\frac{\tau'_{\text{max}}}{\tau'_{\text{min}}}\right)^{2-\alpha'} g(\alpha',\omega_0,\tau'_{\text{max}}) - g(\alpha',\omega_0,\tau'_{\text{min}})\right] \quad (25a)$$

with

$$g(\alpha',\omega_0,\tau'_{\text{max}}) \equiv {}_2F_1\left(1, 1 - \frac{\alpha'}{2}, 2 - \frac{\alpha'}{2}, -\omega_0^2\tau'^2_{\text{max}}\right) \quad (25b)$$

where the hypergeometric function ${}_2F_1$ with these different arguments can also be calculated numerically either by a series or by an asymptotic expression. Substituting eqs 25a and 25b into eq 17 gives

$$R_{Q,\text{Surf-intra}}^{\text{Doublewell}}(\omega_0) = \frac{3}{80}p_B|(\omega_{Q1} - \omega_{Q2})|^2\left(\frac{2\alpha'}{2 - \alpha'}\right)\left(\frac{\alpha}{1 + \alpha}\right) \times \frac{\tau'^2_{\text{min}}}{\tau_{\text{min}}}\left\{\left(\frac{\tau'_{\text{max}}}{\tau'_{\text{min}}}\right)^{2-\alpha'} g(\alpha',\omega_0,\tau'_{\text{max}}) - g(\alpha',\omega_0,\tau'_{\text{min}}) + 4\left[\left(\frac{\tau'_{\text{max}}}{\tau'_{\text{min}}}\right)^{2-\alpha'} g(\alpha',2\omega_0,\tau'_{\text{max}}) - g(\alpha',2\omega_0,\tau'_{\text{min}})\right]\right\} \quad (26)$$

This expression has the two following analytical limits

$$R_{1Q,\text{Surf-intra}}^{\text{Double well}}(\omega_0 \to 0) \approx \frac{3}{8}p_B|(\omega_{Q1} - \omega_{Q2})|^2\left(\frac{\alpha}{1 + \alpha}\right) \times \left(\frac{\alpha'}{2 - \alpha'}\right)\frac{\tau'^2_{\text{min}}}{\tau_{\text{min}}}\left[\left(\frac{\tau'_{\text{max}}}{\tau'_{\text{min}}}\right)^{2-\alpha'} - 1\right] \quad (27a)$$

$$R_{1Q,\text{Surf}-\text{intra}}^{\text{Doublewell}}(\omega_0 \gg 1) \approx \frac{3}{40}p_B|(\omega_{Q1} - \omega_{Q2})|^2\left(\frac{\alpha}{1 + \alpha}\right) \times \left(\frac{\alpha'}{2 - \alpha'}\right)(1 + 2^{\alpha'})\Gamma\left(2 - \frac{\alpha'}{2}\right)\Gamma\left(\frac{\alpha'}{2}\right) \times \frac{\tau'^2_{\text{min}}}{\tau_{\text{min}}}\frac{1}{(\omega_0\tau'_{\text{min}})^{2-\alpha'}} \quad (27b)$$

The low-frequency limit, eq 27a, is a constant as before, while the high-frequency limit, eq 27b, is a power law in the Larmor frequency, $R_{1Q,\text{Surf-intra}}^{\text{Double well}}(\omega_0 \gg 1) \propto 1/\omega_0^{2-\alpha'}$ with a larger exponent that the one obtained at low temperature in eq 20b. Examination of the consequences of this result for the temperature

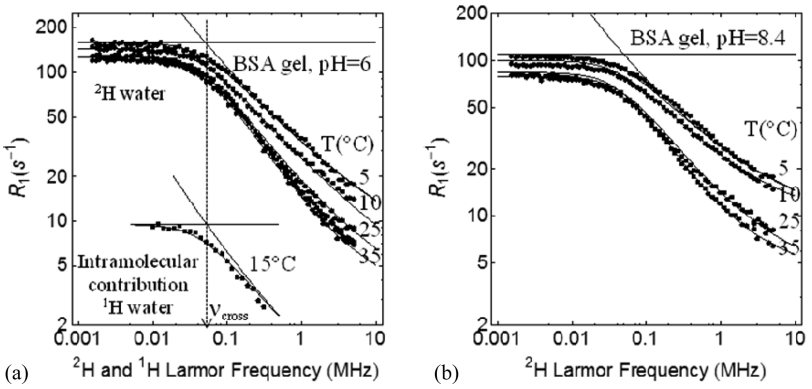

Figure 7. (a) Same legends as Figure 2, but now the continuous lines represent, for the ^{2}H BSA gel data at pH = 6, the best fits obtained with a linear combination of eqs 19 and 26 with $\alpha = 0.52$, $\alpha' = 1.03$, $\omega_{Q1} = 195$ kHz, $\omega_{Q2} = 250$ kHz, and $T = 5-35$ °C. We have also reported the two limits at low and high frequencies. For the intramolecular ^{1}H BSA gel data, the continuous line represents the best fit obtained with eqs 29 and 32 at 15 °C with $\alpha = 0.52$, $E = 4.5$ kcal/mol, $\alpha' = 1.03$, $E' = 3.3$ kcal/mol, $\omega_{D1} = 22.3$ kHz, $\omega_{D2} = 30.5$ kHz, and a τ_{max} value almost equivalent to the one observed for the ^{2}H data, thus proving that the same molecular reorientational dynamics is responsible for the MRD data. (b) Deuteron spin−lattice relaxation rate as a function of the magnetic field strength plotted as the deuteron Larmor frequency for 15% BSA gel in D_2O at pH = 8.4 and at 5, 10, 25, and 35 °C downward. The continuous lines represent the best fits obtained with eq 35 with the same parameters as above.

dependence using eqs 27aand 27b shows that

$$R_{1Q,\,\text{Surf-intra}}^{\text{Doublewell}}(\omega_0, T) \propto \frac{\tau'^{\alpha'}_{\min}(T)}{\tau_{\min}(T)} = \frac{\tau'^{\alpha}_{0}}{\tau_0}\exp\left(\frac{\alpha' E' - E}{RT}\right) \quad (28)$$

in the whole frequency range, if we assume that τ'_{max} is independent of or a very weak function of temperature as we will show below. The energy difference appearing in eq 28 implies a small apparent activation energy for the processes that drive the deuteron relaxation as observed.

We have displayed in Figure 6 the calculated frequency dependences of $f(T)R_{1Q,\text{Surf-intra}}^{\text{Single well}}(\omega_0,T) + [1 - f(T)]R_{1Q,\text{Surf-intra}}^{\text{Double well}}(\omega_0,T)$ obtained with eqs 19 and 26 with $\alpha = 0.52$, $\alpha' = 1.03$, $E = 4.5$ kcal/mol, and $E' = 3.3$ kcal/mol for $T = \{5-35\ °C\}$. Equation 26 tends to eq 19 in the limits where $E' = E$, $\tau' = \tau$ and $\alpha' = \alpha + 1$. Comparison with the data in Figures 2 and 3 shows that these calculations reproduce the net increase of the power-law exponents at high temperature.

3. Proton MRD. The intramolecular part of the water-proton relaxation must be related by a scale factor to the deuterium relaxation rate constant. Using the same theoretical treatment with $I = 1/2$, the dipolar frequency $\omega_D^2 = \gamma^4\hbar^2/r^6$, where $r = 0.158$ nm is the water interproton distance, and the numerical constant 3/10, one obtains the intramolecular surface proton MRD in the single well case

$$R_{1D,\,\text{Surf-intra}}^{\text{Singlewell}}(\omega_0) = \frac{3}{10}p_B\omega_D^2\frac{\alpha}{1-\alpha}\tau_{\min}\left\{\left(\frac{\tau_{\max}}{\tau_{\min}}\right)^{1-\alpha} f(\alpha,\omega_0,\tau_{\max}) - f(\alpha,\omega_0,\tau_{\min}) + 4\left[\left(\frac{\tau_{\max}}{\tau_{\min}}\right)^{1-\alpha} f(\alpha,2\omega_0,\tau_{\max}) - f(\alpha,2\omega_0,\tau_{\min})\right]\right\} \quad (29)$$

This expression can be calculated numerically but has the two following analytical limits

$$R_{1D,\,\text{Surf-intra}}^{\text{Single well}}(\omega_0 \to 0) \approx \frac{3}{2}p_B\omega_D^2\frac{\alpha}{1-\alpha}\tau_{\min}\left[\left(\frac{\tau_{\max}}{\tau_{\min}}\right)^{1-\alpha} - 1\right] = \frac{3}{2}p_B\omega_D^2\langle\tau\rangle \quad (30a)$$

$$R_{1D,\,\text{Surf-intra}}^{\text{Single well}}(\omega_0 \gg 1) \approx \frac{3\pi}{20}p_B\omega_D^2\alpha(1 + 2^{1+\alpha})\sec\left(\frac{\alpha\pi}{2}\right) \times \tau_{\min}\frac{1}{(\omega_0\tau_{\min})^{1-\alpha}} \quad (30b)$$

The direct comparison of eqs 20a and 30a gives the following scaling factor between the low-field relaxation rates for ^{2}H and ^{1}H

$$\frac{R_{1Q,\,\text{Surf-intra}}^{\text{Singlewell}}(\omega_0 \to 0)}{R_{1Q,\,\text{Surf-intra}}^{\text{Singlewell}}(\omega_0 \to 0)} = \frac{\omega_Q^2}{4\omega_D^2} \quad (31)$$

which reproduces quite well the ratio that we observed in Figures 2 and 7a.

For the double well case, one finds similarly

$$R_{1D,\,\text{Surf-intra}}^{\text{Doublewell}}(\omega_0) = \frac{3}{10}p_B|(\omega_{D1} - \omega_{D2})|^2\frac{\alpha}{1+\alpha}\frac{\alpha'}{2-\alpha'} \times\frac{\tau'^2_{\min}}{\tau_{\min}}\left\{\left(\frac{\tau'_{\max}}{\tau'_{\min}}\right)^{2-\alpha'} g(\alpha',\omega_0,\tau'_{\max}) - g(\alpha',\omega_0,\tau'_{\min}) + 4\left[\left(\frac{\tau'_{\max}}{\tau'_{\min}}\right)^{2-\alpha} g(\alpha',2\omega_0,\tau'_{\max}) - g(\alpha',2\omega_0,\tau'_{\min})\right]\right\} \quad (32)$$

There are two asymptotic limits

$$R_{1D,\,\text{Surf-intra}}^{\text{Doublewell}}(\omega_0 \to 0) \approx \frac{3}{2}p_B|(\omega_{D_1} - \omega_{D_2})|^2\frac{\alpha}{1+\alpha}\frac{\alpha'}{2-\alpha'}\frac{\tau'^2_{\min}}{\tau_{\min}} \times\left[\left(\frac{\tau'_{\max}}{\tau'_{\min}}\right)^{2-\alpha'} - 1\right] \quad (33a)$$

$$R_{1D,\,\text{Surf-intra}}^{\text{Doublewell}}(\omega_0 \gg 1) \approx \frac{3}{10}p_B|(\omega_{D_1} - \omega_{D_2})|^2\frac{\alpha}{1+\alpha}\frac{\alpha'}{2-\alpha'} \times(1 + 2^{1+\alpha})\Gamma\left(2-\frac{\alpha'}{2}\right)\Gamma\left(\frac{\alpha'}{2}\right) \times\frac{\tau'^2_{\min}}{\tau_{\min}}\frac{1}{(\omega_0\tau'_{\min})^{2-\alpha'}} \quad (33b)$$

dx.doi.org/10.1021/jp2053426 |J. Phys. Chem. B 2011, 115, 12845–12858

Here again, the direct comparison of eqs 27b and 33b gives the following scaling factor between the high-field relaxation rates for ^{2}H and ^{1}H

$$\frac{R_{1Q,\,\mathrm{Surf\text{-}intra}}^{\mathrm{Doublewell}}(\omega_0 \gg 1)}{R_{1Q,\,\mathrm{Surf\text{-}intra}}^{\mathrm{Doublewell}}(\omega_0 \gg 1)} = \frac{|(\omega_{Q1} - \omega_{Q2})|^2}{4|(\omega_{D_1} - \omega_{D_2})|^2} \tag{34}$$

that reproduces quite well the ratio that we observed in Figures 2 and 7a.

IV. DISCUSSION AND COMPARISON WITH EXPERIMENTS

There are two critical features of these data: (i) At low magnetic fields, the ^2H_2O relaxation rate is independent of field strength, and (ii) the relaxation rate is a power law in the Larmor frequency at higher-field strengths. The low-field plateau may result from two different causes. The correlation between the spins may be interrupted by an exchange event, such as the water molecule leaving the protein interface. In this case, the frequency of the transition to a power law is approximately the reciprocal of the bound-state lifetime. Alternatively, the low-field plateau may derive from local fields dominating the applied magnetic field.[38] At high magnetic field strengths, the effective axis of quantization for the nuclear spins is determined by the applied field, and the Larmor frequency is a linear function of the applied field strength. However, at small values of the applied field strength in systems with solid components, other contributions to the spin Hamiltonian may be important. In the present case, these are the local dipolar field of the protons or the pure nuclear electric quadrupole coupling to the electric field gradient at the deuteron. The magnetic field switches in these experiments are sufficiently slow that the spins adiabatically follow the effective field. At low fields then, the Zeeman contribution may not dominate, and the local field effects can provide a low-field limitation on the effective Larmor frequency. The deuterium quadrupole coupling constant is much larger than the proton−proton dipolar couplings in the present experiments. Therefore, if the low-field plateau was caused by the effects of such local fields, then the transition region for the proton MRD in Figures 2 and 3 would be at much lower field than for the deuterons; however, the transition regions are at the same frequency within experimental error (Figure 2). Therefore, the local-field effects are not the cause of the transition to a plateau at low field. We conclude that the plateau is caused by exchange that interrupts the spin correlations in the bound environment. The reciprocal of the transition frequency, approximately 40 kHz, corresponds to a characteristic time of 2−4 μs, which is remarkably independent of temperature and pH.

An important feature of these data is the independence of the transition frequency to changes in temperature, which is not consistent with the usual activation models for chemical exchange of bound water. However, if the exchange of the rare deeply buried water molecules requires fluctuations of the protein structure to unlock steric constraints, then the exchange and its temperature dependence are controlled by the low-frequency protein dynamics. The ^{1}H MRD of the protein implies that the low-frequency protein fluctuations are described by a fracton model for which the fluctuations that drive the ^{1}H dipolar relaxation are proportional to kT, i.e., linear in the temperature.[30,32] The temperature range of the present experiments is approximately 35°, which corresponds to approximately a 10% change in the temperature. A 10% change in the frequency of the plateau onset is difficult to resolve with the present experiments. Therefore, the approximate independence of the plateau onset is consistent with the protein fluctuations controlling the water exchange rate from the longest-lived protein sites.

At low temperature, the single well model fits the data, but the higher temperature data deviate from the model. Therefore, additional motions contribute to spin relaxation. It is important to note that the foundation for the original description is that the rare sites corresponding to only the deepest free energy minima of Figure 1 dominate the observation. In the vicinity of the extrema, i.e., the deepest wells, the energies are distributed exponentially, which leads directly to the Pareto distribution of correlation times. However, at higher temperature and frequency, one expects contributions from molecular motions corresponding energetically to the area above the shaded region of Figure 1, i.e., not completely dominated by only the deepest wells. There are several ways to incorporate additional dynamics into the relaxation equations; a direct method is to add local bound state motion, i.e., make the bound state a double well minimum with one energy larger than the other as described in Section III.C2 eqs 26 and 27. One may think of this as the second term in an expansion associated with increasingly complex bound-state potential functions; however, we include only up to two unequal wells. We note that at high frequency and high temperature the fast dynamics associated with the vast majority of water in the interfacial region may make a contribution. However, at the very low frequencies of the present experiments, the contributions from this class of reorientational relaxation are small because the correlation times for surface translation and rotation are in the range of tens to hundreds of picoseconds, which lead to effects at much higher frequencies that studied here.

On the basis of all the physical arguments presented above, we propose a linear combination of eqs 19 and 26 to permit quantitative comparison of the theoretical approach outlined above with D_2O MRD profiles.

$$R_{1Q}(\omega_0, T) = f(T)R_{1Q,\,\mathrm{Surf\text{-}intra}}^{\mathrm{Doublewell}}(\omega_0, T) + [1 - f(T)]R_{1Q,\,\mathrm{Surf\text{-}intra}}^{\mathrm{Doublewell}}(\omega_0, T) + R_{1Q,\,\mathrm{Bulk}} \tag{35}$$

where $f(T)$ is a weighting coefficient. The many parameters make a generalized least-squares fit problematic and subject to a number of local minima. However, the low-field plateau and high-field power law provide critical tests of the theory and associated parameters. The solid lines in Figures 7 and 8 are fits to the data of Figures 2 and 3 for BSA and lysozyme at different temperatures and pH with the parameters summarized in the captions. This analysis was developed as follows:

(1) There are several approaches to estimate the probability p_B that a water molecule is in the hydration domain of the protein. One method is to use estimates for the BSA surface area using a water layer thickness of 3 Å, which gives p_B = 0.16 for 15% BSA. A second method is to assume that 0.45 g of water/g of protein is in the interface, which is based on heat capacity changes with hydration and the amount of nonfreezing water.[39] This approximation gives p_B = 0.05 for 15% BSA, which is possibly small. In the following, we choose an intermediate between these two values, p_B = 0.067.

(2) We choose the quadrupole coupling constant for deuterium in D_2O $\omega_Q/2\pi$ = 250 kHz. The magnitude of this coupling constant is a function of the number and

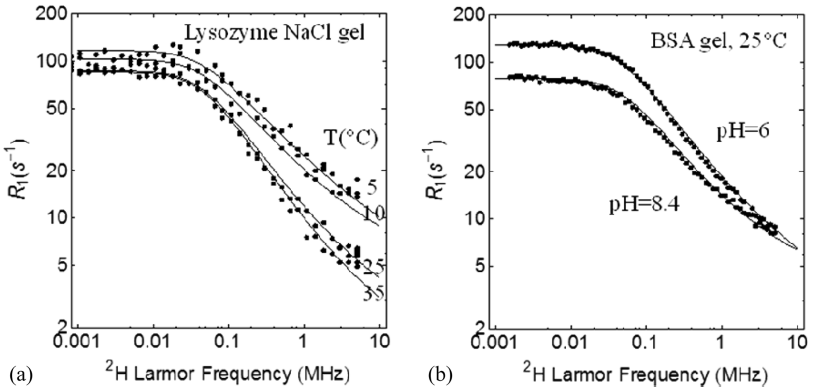

Figure 8. (a) Deuteron spin−lattice relaxation rate as a function of the magnetic field strength plotted as the deuteron Larmor frequency for lysozyme gel in D_2O at 5, 10, 25, and 35 °C, respectively, top to bottom. The continuous lines represent the best fits obtained with eq 35 with the same parameters as described in the legend of Figure 7. (b) Deuteron spin−lattice relaxation rate as a function of the magnetic field strength plotted as the deuteron Larmor frequency for 15% BSA gel in D_2O at pH = 6 and pH = 8.4 at 25 °C. The continuous lines represent the best fits obtained with the same parameters as described in the legend of Figure 7.

geometry of hydrogen bonds formed by the water and may be as small as 240 kHz for water monomers in a nonaqueous solvent.[40−44] The precise value appropriate for protein-bound water is uncertain because binding sites may provide different numbers and geometries of hydrogen bonds.

(3) We fix the Pareto exponent to $\alpha = 0.52$ based on the lowest temperature data in the high-frequency regime (eq 20b), $\omega_0^{-(1-\alpha)}$. According to eq 11, this value for α indicates a very broad distribution of correlation times as shown in Figure 4. If we assume that the hydration domain of BSA includes approximately 1500 water molecules, then there are $1500 \times P_{rest}(\alpha, \tau > \tau_{limit})$ highly trapped water molecules with a correlation time $\tau > \tau_{limit}$. Here, the probability $P_{rest}(\alpha, \tau > \tau_{limit})$ to have a correlation time τ larger than a certain limit τ_{limit} has been calculated with eq 15. When $\alpha = 0.52$, this choice gives 14, 4, and 1 water molecules for $\tau_{limit} \geq 10^4 \cdot \tau_{min}$, $10^5 \cdot \tau_{min}$, and $10^6 \cdot \tau_{min} \approx \tau_{max}$, respectively. These numbers demonstrate that the low-frequency behavior of the spin−lattice relaxation rate is driven by extremely rare interactions. We fix the Pareto exponent for the double well model based on the highest temperature data in the same way.

(4) The activation parameters are selected to give the minimum correlation time for the value of bulk water with activation energies of 4.5 and 3.3 kcal/mol for the single well and double well potential terms, respectively. However, we note that there is justification for the minimum correlation time to be shorter than this based on measurements in nonaqueous solvents.[43]

(5) We take $\tau_{max} \approx 1/(2\pi\nu_{cross}) = 3.0$ μs, corresponding to $1/(2\pi\nu_{cross})$ at the intersection of the two analytical expressions of the plateau at low frequency (eq 20a) and the asymptotic power law at high frequency (eq 20b). We find the same frequency $\nu_{cross} \approx 40$ kHz for ^{2}H and ^{1}H NMRD in BSA gel data (Figure 7a). We emphasize that the data require that τ_{max} is essentially temperature independent.

(6) For the protein-bound state, the quadrupole Hamiltonian for the water deuteron does not average to zero. Because there is not global rotation of the site, the magnitude of the apparent quadrupole contribution to the energy is dependent on orientation in the static magnetic field as well as the degree of local averaging by high-frequency oscillations. The effects of the high-frequency motions may be incorporated by changing the apparent size of the quadrupole coupling constant. For simplicity, we assume that water makes transitions between two different environments with $\omega_{Q1}/2\pi \approx 195$ kHz and $\omega_{Q2}/2\pi = 250$ kHz for BSA gel at pH = 6 and $\omega_{Q1}/2\pi \approx 195$ kHz and $\omega_{Q2}/2\pi = 250$ kHz for BSA gel at pH = 8.4 as well as for the lysozyme gel. With these choices, the highest-temperature experiments may be described well over the whole frequency range with eq 26 and a Pareto exponent $\alpha' = 1.03$.

According to the low-frequency limit given in eq 27a, the fact that $\tau_{max} \approx 2.5$ μs is not very different from the low-temperature results is consistent with the very small temperature effect observed at low frequency (Figure 7). The situation is different in the high-frequency range, where according to the high-frequency asymptotic limit given in eq 27b we have now another power law $1/\omega_0^{(2-\alpha')}$ that has a larger exponent than at low temperature. The value $\alpha' = 1.03$ for BSA gives $1500 \times P_{rest}(\alpha', \tau' > 10\tau'_{min}) \approx 140$ water molecules, i.e., about 9.33% of the water of the hydration domain participates. As seen in Figure 4, the Pareto distribution decays rapidly as a function of the correlation time when $\alpha' = 1.03$.

(7) The apparent value of α may be a function of temperature; however, unless the protein heat capacity is a significant function of temperature over this range, eqs 7 and 8 show that α should not depend significantly on temperature. The protein, however, is a soft solid, and we presume that the populations of double and single well sites are temperature dependent. As a result, we model the complete set of data over all temperatures with fixed parameters and vary only the relative weighting of the single well and double well populations. The results of this approach are summarized in Figures 7 and 8.

(8) Equations 26 and 19 describe the consequences of bound water sites on the total relaxation, and they do not include the effects of diffusion or the other dynamics in the bulk or the interface. The curves shown in Figures 7 and 8 include

an additive constant to account for these contributions that are not modeled in detail here. The constant is larger at high temperature and high pH which is consistent with increasing contributions from the exchange of protein hydroxyl, amide, or amine functions with the water population.

The intramolecular water proton relaxation data are shown in Figure 7a and fit using eqs 16 and 29; the shape and transition frequency agree well with the deuteron results. This agreement is critical. The magnitude of the proton intramolecular relaxation rate also scales correctly to the magnitude of the relaxation rate constants for deuterium as it should. As noted by Halle based on very different experimental approaches,[45] the intramolecular proton relaxation dispersion is different from the total or the intermolecular contributions which usually do not have a sharp low-field plateau. Thus, while the intramolecular contribution to the total proton relaxation is significant, it is not often dominant, in part because for a long-lived water molecule, the distinction between intramolecular and intermolecular contributions is blurred when the rotationally immobilized protons communicate efficiently with each other.

The representation of the data as the sum of two classes of relaxation site contributions is a consistent way to model the data. Both contributions presume a distribution function appropriate to rare events; i.e., the form of the distribution function is related to the exponential distribution of barriers near the extrema represented schematically in Figure 1. Application of the distribution function to the two different spectral density functions, a Lorentzian for the single well, and a modified Lorentzian for the asymmetric double well lead to different power laws in the Larmor frequency. For the single well case, the exponent is $1 - \alpha$, resulting in α significantly less than unity. The consequence of this value is that the correlation time distribution is very wide as shown in Figure 4. The few bound water molecules in the rare sites dominate the low-field relaxation rate constant. In a real sense, the low-field MRD profiles do not represent the dynamics of most water molecules at all. In contrast, the spectral density for the double well model leads to a power-law exponent $2 - \alpha'$ with α' slightly larger than unity. In this case, the correlation time distribution is considerably narrower. Because the difference in activation energies for the local dynamics enters in the double well model relaxation equation, this model accounts for the weak temperature dependence of the relaxation rate in a simple way.

One could assume that the exponent α is temperature dependent because making the relaxation equation a sum of contributions is a way to make the apparent slope of the power law temperature dependent by mixing two contributions with different values for α. The main justification for not adopting this approach is that eqs 8 and 12 imply that the value of α should depend on the square root of the heat capacity, which would imply significant changes in the heat capacity over the 30° range studied. Further, freely adjusting α is insufficient to account for the data at the higher temperatures. Finally, we emphasize that this approach depends on the assumption that the deepest minima of Figure 1 dominate the observations. At much higher magnetic field strengths or Larmor frequencies, additional dynamics are likely to become important, and this approach may be incomplete.

IV. CONCLUSION

The intramolecular contributions to nuclear spin−lattice relaxation rate constants for water in cross-linked protein gels is dominated at low magnetic field strengths, i.e., low Larmor frequencies, by the dynamics of a few rare strongly bound and long-lived water molecules in and on the protein. The dynamics of these few molecules is modeled using extreme-values statistics. We show that the distribution of activation barriers around the minima of the free energy landscape for water interactions is an exponential. This result, combined with the assumption of the usual exponential activation law for motions, leads to a Pareto distribution for the associated correlation times. This correlation time distribution is asymmetrically skewed with a very significant long-time tail that dominates the nuclear spin relaxation at low Larmor frequencies. The exchange of water from the longest lifetime protein sites is limited by or slaved to fluctuations of the protein that depend linearly on the temperature. With increasing temperature, the contributions from increased local motions of water in protein-bound sites are apparent, although the lifetime of the most slowly exchanging water molecules changes little. The spin−lattice relaxation for intramolecular relaxation processes is described well by a theory which follows from the statistics of rare events and is consistent with the fact that the vast majority of the water in the system is characterized by reorientational dynamics that is orders of magnitude faster than the reorientational dynamics of the few molecules that dominate the observation. The fluctuations that permit exchange of water molecules from these rare sites are also rare. Thus, the statistical treatments developed here may have important applications in understanding the long-time parts of the correlation functions for protein dynamics that produce catalytically critical fluctuations.

APPENDIX A

Extreme-Values Statistics. In the following, the probability distribution function, pdf, and cumulative distribution function, cdf, or probability (or repartition function) will be represented by small and capital letters, respectively. Introducing the cdf $F(E)$ defined by

$$F(E) = \int_{-\infty}^{E} p(E')\mathrm{d}E' \tag{A1a}$$

with the pdf given by (eq 1)

$$p(E) = A \exp\left(- \left| \frac{E}{E_0} \right|^{\delta} \right) \tag{A1b}$$

where A and E_0 are defined in eq 1. Equation A1a gives the probability that the random variable E' is lower than E. Similarly, $1 - F(E)$ is the probability that the random variable E' is greater than E.

We are interested in the statistics of the lowest free energy states $E^* = \min\{E_1, \ldots E_i, \ldots E_M\}$ for an ensemble of a very large number of M random variables E_i. In the case of M independent and identically distributed random variables (energies) E_i with $i \in \{1,\ldots,M\}$. E^* is still a random variable with a probability $[1 - F(E^*)]^M$; thus, the positive pdf, $p_M(E^*)$, is given by

$$p_M(E^*) = -\frac{d}{dE^*}[1 - F(E^*)]^M = Mp(E^*)[1 - F(E^*)]^{M-1} \tag{A2}$$

For large M, the minimum E^* will take a large negative value, and the repartition function $F(E^*)$ becomes very small; therefore

$$[1 - F(E^*)]^M \approx \exp[-MF(E^*)] \tag{A3}$$

After substitution of eq A3 into eq A2

$$p_M(E^*) \approx Mp(E^*)\exp[F(E^*)]\exp[-MF(E^*)] \quad \text{(A4)}$$

The repartition function $F(E^*)$ becomes very small when E^* becomes smaller than a characteristic value of free energy, say $E_c(M)$ (Figure 1), defined by the relation: $MF[E_c(M)] = 1$. In consequence, $\exp(F(E^*)) \sim 1$, and eq A4 simplifies

$$p_M(E^*) \approx Mp(E^*)\exp[-MF(E^*)] \quad \text{(A5)}$$

From eq A1, one has

$$MF[E_c(M)] = M\int_{-\infty}^{E_c} p(E')\mathrm{d}E' = 1 \quad \text{(A6)}$$

The integral of eq A6 simplifies when $F(E_c)$ and $p(E_c)$ are very small

$$MF[E_c(M)] = M\Delta E_c(M)p[E_c(M)] = 1 \quad \text{(A7a)}$$

Here, $\Delta E_c(M)$ represents the size of the fluctuations of E^* around $E_c(M)$ (Figure 1). Substituting eq A1b into eq A7a gives

$$p(E_c(M)) = A\exp\left[-\left|\frac{E_c(M)}{E_0}\right|^{\delta}\right] = 1/[M\Delta E_c(M)] \quad \text{(A7b)}$$

In consequence $E_c(M)$ is

$$E_c(M) \approx -E_0(\ln(A\Delta E_c) + \ln(M))^{1/\delta} \approx -E_0(\ln(M))^{1/\delta} \quad \text{(A7c)}$$

when $M \rightarrow \infty$ and considering the fact that $E_c(M)$ is negative. Figure 1 shows that the value of the extreme E^* fluctuates around $E_c(M)$; thus, we expand eq A5 in the neighborhood of $E_c(M)$. We introduce the change of variable

$$E^* = E_c(M) + E^* - E_c(M) = E_c(M)[1 + u_E] \quad \text{(A8a)}$$

With the dimensionless variable

$$u_E = \frac{E^* - E_c(M)}{E_c(M)} \ll 1 \quad \text{(A8b)}$$

With this substitution, the pdf of the extremum E^* given in eq A5 becomes a product of two terms that we will expand in a series of u_E

$$p_M[E^*] \approx (1^{st}\text{ term}) \times (2^{nd}\text{ term})$$
$$(1^{st}\text{ term}) = Mp[E_c(M)(1 + u_E)]$$
$$(2^{nd}\text{ term}) = \exp[-MF[E_c(M)(1 + u_E)]] \quad \text{(A9)}$$

(a). 1st Term of $p_M(E^*)$. Substitution of eq A1b and eq A7b into the first term of eq A9

$$(1^{st}\text{ term}) = MA\exp\left[-\left|\frac{E_c(M)}{E_0}(1 + u_E)\right|^{\delta}\right] \approx \frac{1}{\Delta E_c(M)} \times \exp\left[-\delta u_E\left|\frac{E_c(M)}{E_0}\right|^{\delta}\right] \quad \text{(A10)}$$

Now, we introduce another very small and dimensionless variable u in eq A10 to identify the free energy fluctuation $\Delta E_c(M)$ around $E_c(M)$ (Figure 1)

$$u = \frac{E^* - E_c(M)}{\Delta E_c(M)} = u_E\frac{E_c(M)}{\Delta E_c(M)} \quad \text{(A11)}$$

where the substitution of eq A11 in the last term of eq A10 gives for the first term

$$(1^{st}\text{ term}) = \frac{1}{\Delta E_c(M)}\exp\left[-\delta\left|\frac{E_c(M)}{E_0}\right|^{\delta}u\frac{\Delta E_c(M)}{E_c(M)}\right] \equiv \frac{1}{\Delta E_c(M)}\exp(u) \quad \text{(A12)}$$

Here, the last relation in eq A12 allows definition of the relative fluctuations

$$\frac{\Delta E_c(M)}{E_c(M)} = -\frac{1}{\delta}\left|\frac{E_c(M)}{E_0}\right|^{-\delta} \quad \text{(A13)}$$

Substitution of eq A7c into eq A13 gives the M-dependence of the fluctuation $\Delta E_c(M) > 0$ of free energy around $E_c(M)$

$$\Delta E_c(M) = E_0\frac{(\ln(M))^{(1-\delta)/\delta}}{\delta} \quad \text{(A14)}$$

From eq A14, one sees that the condition $\delta > 1$ is absolutely required to impose that $\Delta E_c(M)$ goes to zero when M goes to infinity; otherwise, the fluctuations will be too large and the distribution of the extremes will diverge. Moreover, by using eq A7c and eq A14, we can estimate how the relative fluctuations $|(\Delta E_c(M))/(E_c(M))|$ decay to zero with increasing M

$$\left|\frac{\Delta E_c(M)}{E_c(M)}\right| \approx \frac{1}{\delta\ln(M)} \quad \text{(A15)}$$

(b). 2nd Term of $p_M(E^*)$. We expand in series the second term of eq A9 using the same method

$$(2^{nd}\text{ term}) \equiv \exp[-MF[E_c(M)(1 + u_E)]] \quad \text{(A16)}$$

The argument of the exponential in eq A16 can be expand in series as

$$MF[E^*] = MF[E_c(M)(1 + u_E)] \approx MF[E_c(M)] + ME_c(M)u_E\frac{dF[E_c(M)]}{dE_c} + \ldots \quad \text{(A17)}$$

Using the change of variables defined in eq A11, with eq A7a, and the definition $MF[E_c(M)] = 1$, eq A17 becomes

$$MF[E^*] \approx 1 + \Delta E_c(M)u[Mp(E_c(M))] + \ldots \approx \exp(+u) \quad \text{(A18)}$$

Substitution of eq A18 into eq A16 thus gives

$$(2^{nd}\text{ term}) \approx \exp[-\exp(u)] \quad \text{(A19)}$$

Now, substitution of eqs A12 and A19 into eq A9 gives finally the pdf distribution known as the universal "*Gumbel" distribution*[29] of

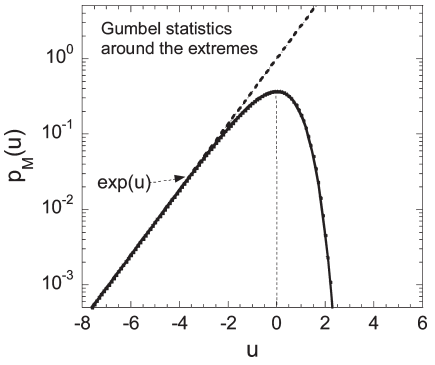

Figure A1. Examples of pdf "Gumbel statistics" of extreme (minimum) $p_M(u)$ calculated from eq 5 or A20 and comparison with an exponential decaying pdf, $\exp(u)$, when $u \rightarrow -\infty$.

the minimum (extreme) of energies expressed in the rescaled minimum free energy variable u and displayed in Figure A1

$$p_M(u) = \frac{1}{\Delta E_c(M)} \exp[u - \exp(u)] \tag{A20}$$

APPENDIX B

Quadrupolar Correlation Function for Water Transitions between Two Different Environments Characterized by Two Wells of Different Activation Energies. We consider the calculation of the correlation function $G_Q(\tau)$ for rare strongly bound D_2O molecules in the protein hydration domain that make random transitions between two potential wells of unequal depths with associated nuclear quadrupole coupling constants, $\omega_{Q1}/2\pi$ and $\omega_{Q2}/2\pi$ ($\omega_{Q1} < \omega_{Q2} = 2\pi \times 240$ kHz, see Figure B1). The calculations can be extended to the intramolecular part of the proton dipolar correlation for H_2O. The two wells are assigned activation energies E' and E ($E' < E$) (Figure B1). The following treatment is an extension of that presented previously by Petit[46] for the case of local ionic motion in solids.

The dynamical information is completely described by the probability to find the water in a given well at a given time τ. We thus omit the tensorial character of the quadrupolar interaction and focus only on the dynamical information that is characterized by the probability $p_i(0)$ for the water molecule to be in the well i at time $t = 0$ and the conditional probabilities $P_{ij}(\tau)$ for the water molecule to be in the well j at a later time t knowing that they start from well i at time $t = 0$. $G_Q(\tau)$ is thus formally given by the relation

$$G_Q(\tau) = \sum_{i=1}^{2} \omega_{Qi} p_i(0) \sum_{j=1}^{2} \omega_{Qj} P_{ij}(\tau) \tag{B1}$$

To take into account the fact that the initial probabilities to be in the well i are not equal, we replace $p_i(0)$ by the equilibrium probability: $p_i(\infty) = \lim_{t\rightarrow\infty} P_{ij}(\tau)$. We thus obtain an averaged quadrupolar correlation function

$$\bar{G}_Q(\tau) = \sum_{i=1}^{2} \omega_{Qi} p_i(\infty) \sum_{j=1}^{2} \omega_{Qj} P_{ij}(\tau) \tag{B2}$$

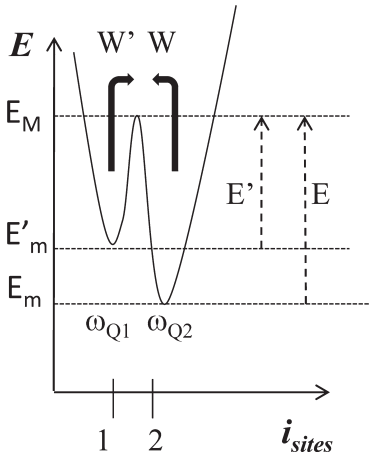

Figure B1. Schematic diagram of the energy landscape around the deepest minimum potential binding sites in the high-temperature limit where the water can explore two quadrupolar environments with unequal wells. All the variables needed for the model described in Appendix B are labeled.

The conditional probabilities $P_{ij}(\tau)$ are solutions of the two coupled kinetic equations

$$\frac{d}{d\tau}\begin{bmatrix} P_{i1}(\tau) \\ P_{i2}(\tau) \end{bmatrix} = -\begin{pmatrix} W & -W' \\ -W & W' \end{pmatrix}\begin{bmatrix} P_{i1}(\tau) \\ P_{i2}(\tau) \end{bmatrix} \tag{B3}$$

where W' and W represent the transition rates coming from sites 1 and 2, respectively (Figure B1). These transition rates follow activation laws related to the respective activation energies of the two wells

$$W = W_0 \exp\left(-\frac{E}{RT}\right),\ W' = W_0' \exp\left(-\frac{E'}{RT}\right) \tag{B4}$$

The hypothesis that the water molecule stays initially on one of the two wells, namely, if $i = 1$, $P_{11}(0) = 1$, $P_{12}(0) = 0$ and if $i = 2$, $P_{21}(0) = 0$, $P_{22}(0) = 1$, it allows us to find the four different solutions of eq B3

$$\begin{aligned} P_{11}(\tau) &= \frac{1}{W + W'}[W' + We^{-(W + W')\tau}], \\ P_{12}(\tau) &= \frac{W}{W + W'}[1 - e^{-(W + W')\tau}], \\ P_{12}(\tau) &= \frac{W'}{W + W'}[1 - e^{-(W + W')\tau}], \\ P_{22}(\tau) &= \frac{1}{W + W'}[W + W'e^{-(W + W')\tau}] \end{aligned} \tag{B5}$$

From eqs B5, one finds the probability of occupancy of each site at equilibrium

$$\begin{aligned} p_1(\infty) &= \lim_{t\rightarrow\infty} P_{11}(\tau) = \frac{W'}{W + W'}, \\ p_2(\infty) &= \lim_{t\rightarrow\infty} P_{22}(\tau) = \frac{W}{W + W'} \end{aligned} \tag{B6}$$

which obeys the conservation relation

$$p_1(\infty) + p_2(\infty) = 1 \tag{B7}$$

Substituting eqs B5 and eqs B6 into eq B2 gives

$$\bar{G}_Q(\tau) = \left[\omega_{Q1}\frac{W'}{W + W'} + \omega_{Q2}\frac{W}{W + W'}\right]^2 + |(\omega_{Q1} - \omega_{Q2})|^2\frac{WW'}{(W + W')^2}e^{-(W + W')\tau} \quad \text{(B8)}$$

Introducing the correlation times

$$\tau = \frac{1}{W} = \tau_0 \exp\left(\frac{E}{RT}\right), \tau' = \frac{1}{W'} = \tau_0' \exp\left(\frac{E'}{RT}\right),$$
$$\tau_p = \frac{1}{W + W'} = \frac{\tau\tau'}{\tau + \tau'} \quad \text{(B9)}$$

one finds finally the following averaged correlation function and spectral density

$$\bar{G}_Q(\tau) = \left[\omega_{Q1}\frac{\tau}{\tau + \tau'} + \omega_{Q2}\frac{\tau'}{\tau + \tau'}\right]^2 + |(\omega_{Q1} - \omega_{Q2})|^2\frac{\tau_p}{\tau + \tau'}e^{-\tau/\tau_p} \quad \text{(B10)}$$

$$J_Q(\omega_0) = 2|(\omega_{Q1} - \omega_{Q2})|^2\frac{1}{\tau + \tau'}\frac{\tau_p^2}{1 + \omega_0^2\tau_p^2} \quad \text{(B11)}$$

AUTHOR INFORMATION

Corresponding Author
*E-mail: rgb4g@virginia.edu. Phone: 1-434-924-1494.

ACKNOWLEDGMENT

The authors acknowledge support from the National Institutes of Health, USA, The University of Virginia, The CNRS, and the Ecole Polytechnique, Palaiseau. We are grateful for helpful discussions with Pierre Levitz, Denis Grebenkov, Yosse Klafter, and Maurice Goldman.

REFERENCES

(1) Kimmich, R.; Anoardo, E. *Prog. Nucl. Magn. Reson. Spectrosc.* **2004**, *44*, 257–320.
(2) Prabhu, N.; Sharp, K. *Chem. Rev.* **2006**, *106*, 1616–1623.
(3) Kumar, P.; Franzese, G.; Buldgrev, S. V.; Stanley, H. E. *Lect. Notes Phys.* **2008**, *752*, 3–22.
(4) Kamal, J. K. A.; Zhao, L.; Zewail, A. H. *Proc. Natl. Acad. Sci. U.S.A.* **2004**, *101*, 13411–13416.
(5) Marchi, M.; Sterpone, F.; Ceccarelli, M. *J. Am. Chem. Soc.* **2002**, *124*, 6787–6791.
(6) Pizzitutti, F.; Marchi, M.; Sterpone, F.; Rossky, P. J. *J. Phys. Chem. B* **2007**, *111*, 7584–7590.
(7) Chen, S.-H.; Lagi, M.; Chu, X.-Q.; Zhang, Y.; Kim, C.; Faracone, A.; Fratini, E.; Baglioni, P. *Spectroscopy* **2010**, *24*, 1–24.
(8) Nakasako, M. *J. Biol. Phys.* **2002**, *28*, 129–137.
(9) Pal, S. K.; Peon, J.; Bagchi, B.; Zewail, A. H. *J. Phys. Chem. B* **2002**, *106*, 12376–12395.
(10) Pal, S. K.; Peon, J.; Zewail, A. H. *Proc. Natl. Acad. Sci. U.S.A.* **2002**, *99*, 1763–1768.
(11) Pal, S. K.; Zewail, A. H. *Chem. Rev.* **2004**, *104*, 2099–2123.
(12) Kwon, O.-H.; Yoo, T. H.; Othon, C. M.; Van Deventer, J. A.; Tirrell, D. A.; Zewail, A. H. *Proc. Natl. Acad. Sci. U.S.A.* **2010**, *107*, 17101–17106.
(13) Zhong, D.; Pal, S. K.; Zewail, A. H. *Chem. Phys. Lett.* **2011**, *503*, 1–11.
(14) Grebenkov, D. S.; Goddard, Y. A.; Diakova, G.; Korb, J.-P.; Bryant, R. G. *J. Phys. Chem. B* **2009**, *113*, 13347–13356.
(15) Kimmich, R.; Klammler, F.; Skirda, V. D.; Serebrennikova, I. A.; Maklakov, A. I.; Fatkullin, N. *Appl. Magn. Reson.* **1993**, *4*, 425–440.
(16) Kimmich, R.; Nusser, W.; Gneiting, T. *Colloids Surf.* **1990**, *45*, 283–302.
(17) Kimmich, R.; Weber, H. W. *Phys. Rev. B: Condens. Matter* **1993**, *47*, 11788–11794.
(18) Nusser, W.; Kimmich, R. *J. Phys. Chem. A* **1990**, *94*, 5637–5639.
(19) Mattea, C.; Qvist, J.; Halle, B. *Biophys. J.* **2008**, *95*, 2951–2963.
(20) Makarov, V. A.; Kim, B.; Andrews, P. E.; Pettit, B. M. *Biophys. J.* **2000**, *79*, 2966–2974.
(21) Denisov, V. P.; Halle, B. *Faraday Discuss* **1996**, *103*, 227–244.
(22) Halle, B.; Denisov, V. P.; Venu, K. In *Biol. Magn. Reson.*; Krishna, N. R., Berliner, L. J., Ed.; Plenum Press: New York, 1999; Vol. 17, pp 419−484.
(23) Halle, B. *Philos. Trans. R. Soc. Ser. B* **2004**, *359*, 1207–1224.
(24) Kiihne, S.; Bryant, R. G. *Biophys. J.* **2000**, *78*, 2163–2169.
(25) Van-Quynh, A.; Willson, S.; Bryant, R. G. *Biophy. J.* **2003**, *84*, 558–563.
(26) Denisov, V. P.; Peters, J.; Horlein Hans, D.; Halle, B. *Biochemistry* **2004**, *43*, 12020–12027.
(27) Otting, G.; Liepinsh, E.; Farmer, B. T., 2nd; Wuthrich, K. *J. Biomol. NMR* **1991**, *1*, 209–215.
(28) Otting, G.; Liepinsh, E.; Wuthrich, K. *Science* **1991**, *254*, 974–980.
(29) Gumbel, E. J. *Statistics of Extremes*; Columbia University Press: New York, 1958.
(30) Korb, J. P.; Bryant, R. G. *J. Chem. Phys.* **2001**, *115*, 10964–10974.
(31) Korb, J. P.; Bryant, R. G. *Magn. Reson. Med.* **2002**, *48*, 21–26.
(32) Korb, J.-P.; Bryant, R. G. *Biophys. J.* **2005**, *89*, 2685–2692.
(33) Halle, B.; Davidovic, M. *Proc. Natl. Acad Sci. U.S.A.* **2003**, *100*, 12135–12140.
(34) Koenig, S. H.; Schillinger, W. E. *J. Biol. Chem.* **1969**, *244*, 3283–3289.
(35) Qvist, J.; Persson, E.; Mattea, C.; Halle, B. *Faraday Discuss.* **2009**, *141*, 131–144.
(36) Bouchaud, J.-P.; Mezard, M. *J. Phys. A: Math. Gen.* **1997**, *30*, 7997–8015.
(37) Abragam, A. *The Priniciples of Nuclear Magnetism*; Oxford University Press: Oxford, 1961.
(38) Kimmich, R.; Schnur, G.; Scheuermann, A. *Chem. Phys. Lipids* **1983**, *32*, 271–322.
(39) Kuntz, I. D. J.; Brassfield, T. S.; Law, G. D.; Purcell, G. V. *Science* **1969**, *163*, 1329–1331.
(40) Alfredsson, M.; Hermansson, K. *Chem. Phys.* **1999**, *242*, 161–175.
(41) Cummins, P. L.; Bacskay, G. B.; Hush, N. S.; Halle, B.; Engstroem, S. *J. Chem. Phys.* **1985**, *82*, 2002–2013.
(42) Farrar, T. C.; Ropp, J. A. *J. Mol. Liq.* **2002**, *98−99*, 103–127.
(43) Goodnough, J. A.; Goodrich, L.; Farrar, T. C. *J. Phys. Chem. A* **2007**, *111*, 6146–6150.
(44) Ludwig, R.; Weinhold, F.; Farrar, T. C. *J. Chem. Phys.* **1995**, *103*, 6941–6950.
(45) Sunde, E. P.; Halle, B. *J. Am. Chem. Soc.* **2009**, *131*, 18214–18215.
(46) Petit, D. *Specific aspects of magnetic resonance of quadrupolar nuclei. Application to the study of "nasicon" solid electrolytes*; Ph.D. Thesis, University of Paris-Sud Orsay, 1987.